Jurnal Teknologi

Full Paper

DESIGN AND ANALYSIS OF A MULTI-ARRAY AND OVERLAPPING CONNECTION USING PIEZOELECTRIC ENERGY HARVESTER

Nik Ahmad Kamil Zainal Abidin, Norkharziana Mohd Nayan*, Nursabirah Jamel, Azuwa Ali, Fatin Farah Farhana Zalnal

Fakulti Teknologi Kejuruteraan Elektrik (FTKE), Universiti Malaysia Perlis, Pauh Putra Campus, 02600 Arau, Perlis, Malaysia

Article history
Received
15 May 2024
Received in revised form
19 February 2025
Accepted
23 February 2025
Published Online
24 October 2025

*Corresponding author
norkharziana@unimap.edu.my

Graphical abstract

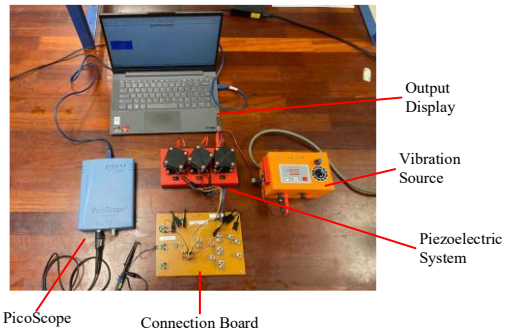

Abstract

There has been much research done on energy harvesting by capturing vibration from low frequency energy. In essence, an array of piezoelectric connections is used to convert kinetic energy into electrical energy in order to produce low frequency energy. This paper presents an investigation on vibration energy harvesting which compares the performances of array piezoelectric connection. This research utilized maximum three pieces of circular piezoelectric sensor which adequate to test the combinations of array connection. Selection of the piezoelectric sensor array are series, parallel, series-parallel, parallel-series and overlapping. The observation is finding the highest power output between array piezoelectric connections. The result show that 3P piezoelectric connection obtained a higher power output among the other types of array piezoelectric which was 3.12 mW.

Keywords: Piezoelectric, energy harvesting system, kinetic energy, multi-array, overlapping

Abstrak

Terdapat banyak kajian yang telah dilakukan mengenai penjanaan tenaga dengan menangkap getaran daripada tenaga frekuensi rendah. Secara asasnya, satu rangkaian sambungan piezoelektrik digunakan untuk menukar tenaga kinetik kepada tenaga elektrik bagi menghasilkan tenaga frekuensi rendah. Kertas ini membentangkan satu penyelidikan mengenai penjanaan tenaga getaran yang membandingkan prestasi rangkaian sambungan piezoelektrik. Penyelidikan ini menggunakan maksimum tiga keping sensor piezoelektrik bulat yang mencukupi untuk menguji kombinasi rangkaian sambungan. Pemilihan rangkaian sambungan sensor piezoelektrik adalah secara siri, selari, siri-selari, selari-siri, dan bertindih. Pemerhatian adalah untuk mencari output kuasa tertinggi antara sambungan rangkaian piezoelektrik. Hasil menunjukkan bahawa sambungan piezoelektrik 3P menghasilkan output kuasa lebih tinggi berbanding jenis rangkaian lain, iaitu sebanyak 3.12 mW.

Kata kunci: Piezoelektrik, sistem penuaian tenaga, tenaga kinetic, pelbagai susunan, bertindih

1.0 INTRODUCTION

The increasing demand for wireless electronic generation has led to major progress in energy harvesting systems in recent years [1]. Energy can be harvested from a variety of environmental sources such as human movement and vibrations [2], [3], [4], [5], [6]. Utilizing the energy supplies that are accessible helps to encourage sustainable development by reducing dependent on traditional batteries.

Piezoelectric energy harvesting can be used to extract mechanical energy from a range of sources, such as sound waves, human movement and low-frequency seismic vibrations [7], [8], and [9]. This energy may be effectively converted into useable electrical energy, which opens up applications in a range of industries, such as industrial actuators, medical sensors, and microphones. Moreover, piezoelectric energy harvesting can be used to directly power consumer gadgets like cell phones, two-way communicators, and pagers [10], [11], [12], and [13].

A simple method for capturing mechanical energy from the environment and converting it into electrical power is using piezoelectric energy harvesting [6]. Due to the piezoelectric effect is exclusive to a material and depends only on its intrinsic polarization, it does not require contact with other components, an external voltage source, or a magnetic field [14], [15], [16]. Effective energy harvesting is made possible by the piezoelectric phenomenon, which transforms mechanical strain into electrical voltage.

Numerous analysis methods have been proposed to design and evaluate energy harvesting systems incorporating multiple arrays and overlapping connections of piezoelectric transducers [16], [17], [18], [19]. In alignment with these methodologies, the main objective of this research is to develop a multi-array configuration and integrate an overlapping connection of piezoelectric transducers, creating an efficient energy harvesting system.

The main objective is to analyze and evaluate the output performance of the developed system, specifically its efficiency and effectiveness in converting mechanical vibrations into usable electrical energy. Through the analysis of output results, valuable insights can be obtained regarding the system's performance and its potential practical applications, particularly in harnessing ambient vibrations as a sustainable energy source [20], [21], [22].

1.1 Energy Harvesting Source

The process of collecting and converting energy from sources including mechanical loads, vibrations, temperature gradients, and light, among others, is known as energy harvesting. The result is often very low total power. Energy can be harvested from motion, temperature gradients, light, electromagnetic radiation, chemical energy and more. Three alternative transduction processes, electromagnetic, electrostatic, and piezoelectric transduction, are accessible for motion. Energy harvesting is important because it provides an alternative source of electricity for electronic devices in areas without access to conventional energy sources [23].

1.2 History and Development of Piezoelectric

Curie's discovery of the piezoelectric phenomenon marked the recognition of the relationship between pressure and electricity, with the term "piezo" meaning pressure and "electric" referring to electricity. When the crystal is subjected to pressure, an electric field is produced, resulting in the observation of a voltage, known as the piezoelectric effect. Initially, the practical use of this effect was limited due to the small electric field it produced. However, with the introduction of LiTiBa ceramics, piezoelectric performance has improved significantly, making it a commonly used electrical component.

Piezoelectric materials exhibit bidirectional behavior, allowing the conversion of both mechanical deflection or force and electrical power. To increase deflection, stacked or bent devices are used, especially in sensor applications that use conventional diaphragm or spring mass damper designs. The market offers different types of piezoelectric sensors, such as strip and circular types show in Figure 1 and 2, each with different frequency characteristics and output values. Typically, piezoelectric sensors produce a higher voltage output and a lower current output [24]

Figure 1 Strip piezoelectric sensor

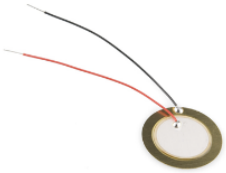

Figure 2 Circular piezoelectric sensor

Piezoelectricity is exhibited by crystals made of dielectric material, where the application of pressure results in the conversion of kinetic energy into electrical energy. When pressure is applied to a dielectric material, it produces an electric field. Polarized molecules in the material respond to the

electric field, creating dipoles and causing changes in the material's dimensions. This phenomenon is known as the piezoelectric effect.

In piezoelectric vibrations, specific equations describe the relationship between voltage, charge and mechanical stress or strain in Figure 3. Piezoelectric vibration analysis starts with this equation [3]. When pressure is applied to a dielectric substance, an electric field is created which results in the production of voltage. The applied pressure affects the output voltage's magnitude; higher pressure results in a higher voltage output [25].

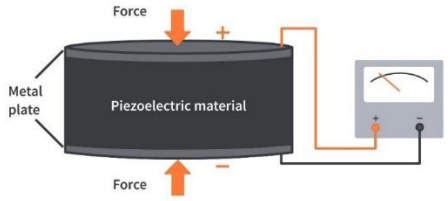

Figure 3 Working Principle Piezoelectric

1.3 Piezoelectricity Theory

The generating of electric charge (Q) in response to mechanical stress (S) or strain (ε) is known as the piezoelectric effect. The piezoelectric coefficient is commonly used to quantify this effect (d). This is the piezoelectric effect equation,

$$Q = d * S \tag{1}$$

The force exerted per unit area is known as mechanical stress (S), and the subsequent deformation or change in dimensions is known as strain (ε). The elastic modulus (E) of the material describes the connection between stress and strain. The formula for calculating mechanical stress is as follows,

$$S = E * \varepsilon \tag{2}$$

The applied mechanical stress or strain is directly proportional to the voltage (V) generated across a piezoelectric material. The coefficient of piezoelectric voltage (g) is the proportionality constant. The voltage generated is computed using the following formula,

$$V = g * S = g * (E * \varepsilon) \tag{3}$$

In piezoelectric materials, the relationship between mechanical stress or strain and the corresponding electrical charge or voltage can be understood using these equations as a basic framework. The specific coefficients (d and g) depend on the material properties of the piezoelectric material being used and can vary for different materials.

2.0 METHODOLOGY

2.1 Block Diagram

The system starts by harvesting vibrations into piezoelectric. Vibration energy will be converted into electrical energy through a piezoelectric sensor. The voltage form for the current is the AC voltage form. To convert the generated AC voltage form into a DC voltage form, an AC-DC converter circuit is therefore required. The energy harvesting system based on piezoelectric sensors is shown in the block diagram in Figure 4. The focus is multi-array and overlapping connections for piezoelectric sensor. Several array topologies have been investigated for piezoelectric sensor arrays at the harvesting stage, including series, parallel, series-parallel and parallel-series combinations. A new positive and negative connection is added to the piezoelectric sensor for overlapping design. This is to study the effect of the output when added a new connection on the piezoelectric.

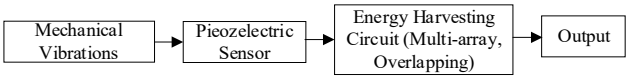

Figure 4 Block Diagram

2.2 Experimental System Block Diagram

Figure 5 shows block diagram of an experimental system that consisting of multiple components on the system that working together to investigate vibration effects. The system starts with a vibration motor controlled by a PWM controller, powered by a 10V supply, and uses different PWM settings (40%, 50%, 60%) for testing to create several types of vibration. At 40%, the motor produces lower-intensity vibrations. Increasing to 50% provides mid-range vibrations with moderate intensity and stability, while 60% results in stronger, more pronounced vibrations. The resulting vibrations are sent to the piezoelectric system, acting as an input for the connection board. The connection board allows configuration control, offering options such as series, parallel, multi-array and overlapping connections, facilitated by integrated switches. The output from the connection board is observed using a PicoScope or similar device, allowing monitoring and analysis of output waveforms and voltage levels.

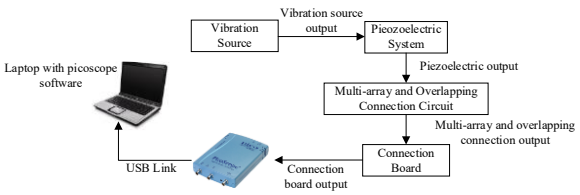

Figure 5 Experimental System Block Diagram

2.3 Array and Overlapping Configuration

Circular piezoelectric sensors are used to test several types of connection circuits during experiments. All types of circuits are given the same pressure method on the piezoelectric by using the vibration method of the piezoelectric surface using vibration motor. The purpose of this experiment is to collect voltage data for each type of circuit.

In order to show the behavior of two piezoelectric plates, a single voltage value was applied, and the output charges produced by the piezoelectric plates were restored to be Q1, Q2. The parallel (b) and series (a) connection arrangements are displayed in Figure 6. The global output voltage in a series connection is the total of all the output voltages, as shown in equation (3), whereas the global output charge in a series connection is equal to each output charge produced by each piezoelectric plate, Q = Q1 = Q2.

$$V = V_1 + V_2 \tag{4}$$

$$V_1 = \frac{Q}{C_{p1}}, V_2 = \frac{Q}{C_{p2}} \tag{5}$$

In terms of electrical current, I flowing through the external load R as in equation (4) below

$$I_p = \frac{V}{R} = \frac{(V_1 + V_2)}{R} \tag{6}$$

Under the assumption of equal piezoelectric materials, that is, $C_{p1} = C_{p2}$ and $V_1 = V_2$ leading to equation (5):

$$C_p = \frac{C_{p1}}{2} = \frac{C_{p2}}{2} \tag{7}$$

Conversely, in parallel connection the global output charge is the sum of each output charge generated by each piezoelectric plates, $Q=Q_1+Q_2$, whereas the global output voltage is equal to each output voltage, that is, $V=V_1=V_2$. By following the same procedure discussed for series connection the total capacitance is, $C_P=C_{P1}+C_{P2}$. Where Pout is the electrical output power, defined as equation (6),

$$P_{out} = VI_p \tag{8}$$

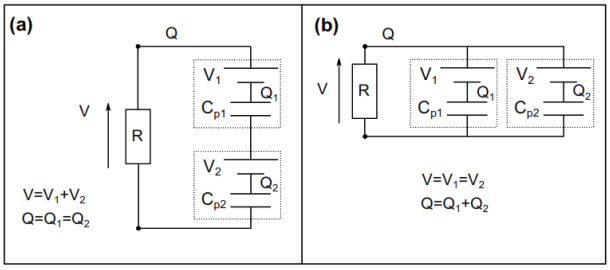

Figure 6 a) Series connection of two piezoelectric plates. (b) Parallel connection of two piezoelectric plates. V and Q represent the global output voltage and output charge, respectively, R is the external load [26]

2.3.1 1-Series Piezoelectric (1S)

This circuit involves only one piezoelectric sensor show in Figure 7 that is connected in parallel with resistor. The purpose of this connection being tested is to make the result to be a reference to other connections. The positive terminal resistor connects to the positive probe and the negative terminal connects to the negative probe PicoScope.

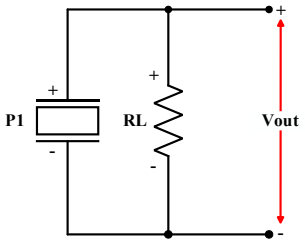

Figure 7 1-Series Circuit

2.3.2 2-Series Piezoelectric (2S)

2-Series Piezoelectric uses two piezoelectric sensor connected in series. As Figure 8 below, piezoelectric 1 and piezoelectric 2 are connected in parallel with resistor. Positive terminal piezoelectric 1 connects to positive terminal resistor. While, negative piezoelectric 2 connects to negative terminal resistor. Then, the positive terminal resistor connects to the positive probe and the negative terminal connects to the negative probe PicoScope.

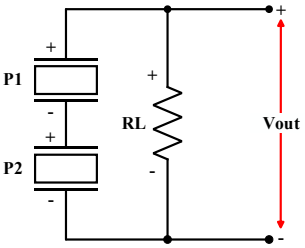

Figure 8 2-Series Circuit

2.3.3 3-Series Piezoelectric (3S)

This 3-Series Piezoelectric circuit uses three piezoelectric sensors used in series connection in Figure 9. Positive terminal piezoelectric 1 is connected to the positive terminal resistor. Meanwhile, the negative terminal piezoelectric 3 is connected to the negative terminal resistor. Then, the positive terminal resistor connects to the positive probe and the negative terminal connects to the negative probe PicoScope.

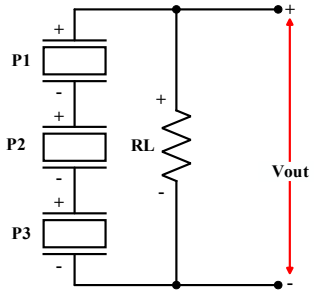

Figure 9 3-Series Circuit

2.3.4 2-Parallel (2P)

This 2-Parallel Piezoelectric circuit uses two piezoelectric sensors connected in parallel in Figure 10. Both positive and negative terminals for piezoelectric 1 and piezoelectric 2 are connected to the positive and negative terminal resistor. Then, the positive terminal resistor connects to the positive probe and the negative terminal connects to the negative probe PicoScope.

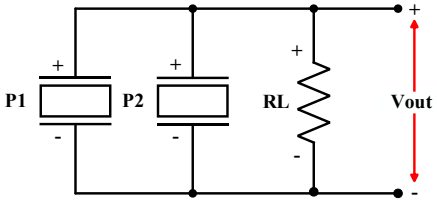

Figure 10 2-Parallel Circuit

2.3.5 3-Parallel (3P)

3-Parallel Piezoelectric uses three piezoelectric sensors connected in parallel in Figure 11. Positive and negative terminals for piezoelectric 1, piezoelectric 2 and piezoelectric 3 are connected to the positive and negative terminal resistor. Then, the positive terminal resistor connects to the positive probe and the negative terminal connects to the negative probe PicoScope.

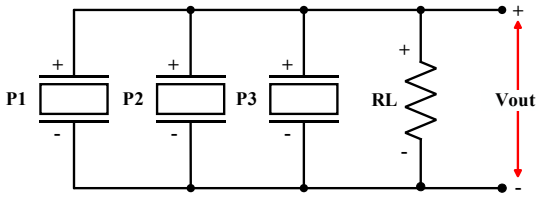

Figure 11 3-Parallel Circuit

2.3.6 2-Series-1-Parallel (2S-1P)

2-Series-1-Parallel Piezoelectric connection show in Figure 12 is a multiarray connection that involves three pieces piezoelectric. Piezoelectric 1 and piezoelectric 2 is connected in series. While, piezoelectric 3 is parallel with piezoelectric 1 and piezoelectric 2. Then, the connection is parallel also with resistor. The positive terminal resistor connects to the positive probe and the negative terminal connects to the negative probe PicoScope.

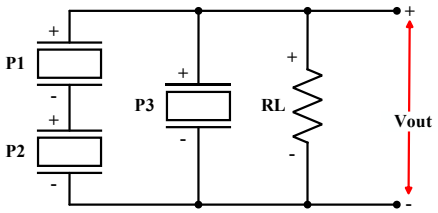

Figure 12 2-Series-1-Parallel Circuit

2.3.7 2-Parallel-1-Series (2P-1S)

2 Parallel 1 Series connection is also a multi-array connection that involves three pieces piezoelectric in Figure 13. Piezoelectric 1 and piezoelectric 2 that connect in series are parallel with piezoelectric 3. Then, the connection is parallel with resistor. The positive terminal resistor connects to the positive probe and the negative terminal connects to the negative probe PicoScope.

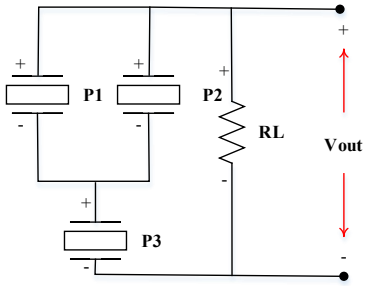

Figure 13 2-Parallel-1-Series Circuit

2.3.8 3-Series-Positive-Overlapping

Overlapping involves connecting a piezoelectric with another piezoelectric, adding an extra positive terminal to create a positive or negative connection. Typically, piezoelectric have one positive and one negative terminal. With the overlapping method, an additional positive terminal is introduced to one piezoelectric and connected to the other. In Figure 14, an overlapping connection is shown with three piezoelectric connected in series. Piezoelectric 1 has an added positive terminal connected to the positive terminal of piezoelectric 2. Similarly, piezoelectric 2 has an added positive terminal connected to the positive terminal of piezoelectric 3. The connection is then made in parallel with a resistor. The positive terminal of the resistor is connected to the positive probe, while the negative terminal is connected to the negative probe of the PicoScope.

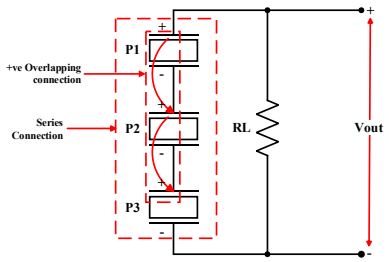

Figure 14 3-Series-Positive-Overlapping Circuit

2.3.9 3-Series-Negative-Overlapping

Series overlapping negative in Figure 15 involves three pieces piezoelectric in series connection. Piezoelectric 1 has been added another negative terminal and connected to the negative terminal of piezoelectric 2. Same as piezoelectric 2 has been added another negative terminal and connected to the negative terminal of piezoelectric 3. Then, the connection is parallel with resistor. The positive terminal resistor connects to the positive probe and the negative terminal connects to the negative probe PicoScope.

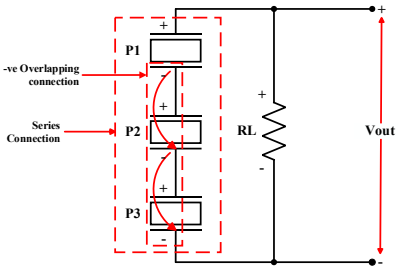

Figure 15 3-Series-Negative-Overlapping Circuit

2.3.10 3-Parallel-Positive Overlapping

Parallel overlapping positive show in Figure 16 involves three pieces piezoelectric in parallel connection. Piezoelectric 1 has been added another positive terminal and connected to the positive terminal of piezoelectric 2. Same as piezoelectric 2 has been added another positive terminal and connected to the positive terminal of piezoelectric 3. Then, the connection is parallel with resistor. The positive terminal resistor connects to the positive probe and the negative terminal connects to the negative probe PicoScope.

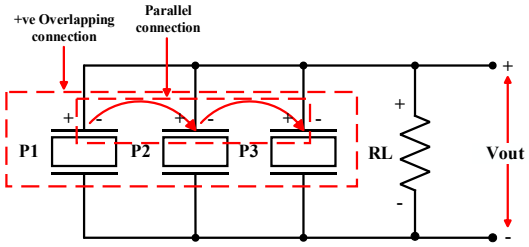

Figure 16 3-Parallel-Positive-Overlapping Circuit

2.3.11 3-Parallel-Negative-Overlapping

Parallel overlapping negative in Figure 17 involves three pieces piezoelectric in parallel connection. Piezoelectric 1 has been added another negative terminal and connected to the negative terminal of piezoelectric 2. Same as piezoelectric 2 has been added another negative terminal and connected to the negative terminal of piezoelectric 3. Then, the connection is parallel with resistor. The positive terminal resistor connects to the positive probe and the negative terminal connects to the negative probe PicoScope.

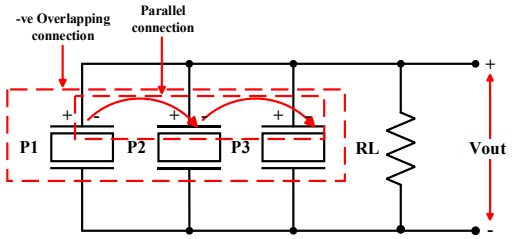

Figure 17 3-Parallel-Negative-Overlapping Circuit

2.4 Experimental Setup

Figure 18 shows the piezoelectric system involves three circular piezoelectric pieces which 35mm diameter each inserted into the prototype, serving as the main component to convert mechanical vibrations into electrical charges. The connection board allows flexible configurations such as series, parallel, multi-array and overlapping circuits by modifying the connection circuit using buttons. A vibration motor with a DC 5V power supply acts as a vibration source input, generating mechanical vibration. The piezoelectric piece then converts these vibrations into a corresponding electrical charge. PicoScope 4262 Analogue PC Based Oscilloscope with 2 analog channels and 5MHz bandwidth is used to measure voltage waves produced by piezoelectric systems. An oscilloscope accurately captures the electrical signals produced by the piezoelectric pieces. The output display visually represents the voltage and frequency outputs from the experimental setup, providing a clear picture of the collected data.

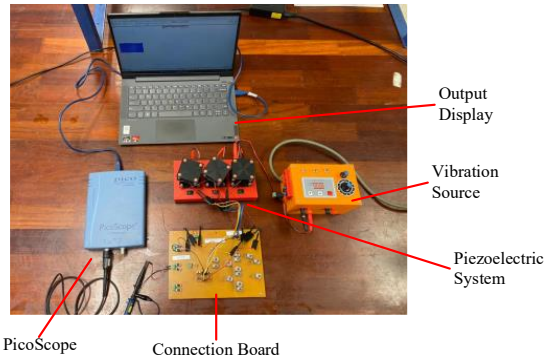

Figure 18 Piezoelectric System

2.4.1 Piezoelectric System

Figure 19 shows the piezoelectric system designed with three sets of piezoelectric as its main component. Each set comprises a vibration motor, which plays a significant role in generating vibrations. The motor is connected to a vibration source, and the speed of the motor is precisely controlled by the vibration source itself. A separate on/off button motor is included with every set of piezoelectric in the system to facilitate easy control. Due to this architecture, users can separately turn on and off each set, giving the system operation flexibility and personalization.

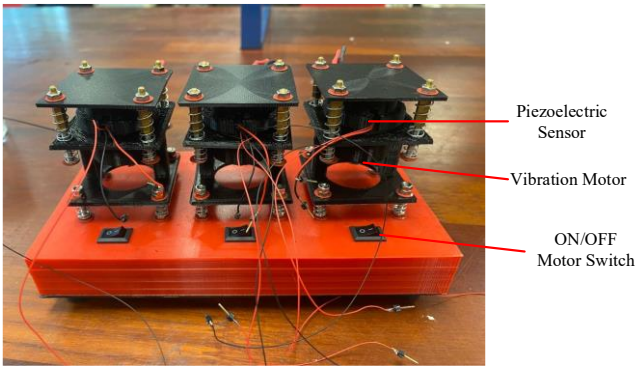

Figure 19 Piezoelectric System

2.4.2 Connection Board

Within the experimental arrangement, the connection board plays a crucial role. It serves as a control mechanism for the system's overlapping, multi-array, parallel, and series connections. The original board, as show in Figure 20, which has 13 buttons that are specifically made for connection control, providing a wide range of configuration possibilities.

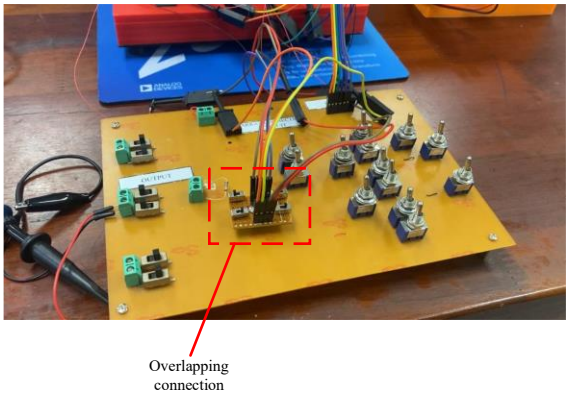

Figure 20 Connection Board

Four additional buttons have been added to the board to improve its usefulness and allow for overlapping connections. There are two of these extra buttons for positive overlapping connections (PO) and two for negative overlapping connections (NO). Furthermore, six buttons are devoted to controlling the output. The board also has an input 6-pin female header, which allows the piezoelectric system to be connected as the input source. The connection board as a whole ensures effective integration of the piezoelectric system into the entire experimental setup by offering the control and flexibility required to build various connection configurations.

3.0 RESULTS AND DISCUSSION

3.1 Experimental Result

In this experiment, the output voltage and power of a piezoelectric vibration device are measured. To test this parameter, a 10M ohm load resistor is connected in parallel with the system. Three distinct speeds are applied to the system: 40%, 50%, and 60%. These speeds are managed by a Pulse Width Modulation (PWM) generator. The electrical energy needed for vibration is provided by a piezoelectric device that is coupled to a reliable power source.

3.1.1 Series of Piezoelectric Configuration System Experimental Result

Piezoelectric devices were used in the experiment to test various connection arrangements. When a single element is linked in series in a 1S connection, the output voltage, and power are at their lowest at 40% speed and at their maximum at 60% speed. When two elements are connected in series in a 2S connection, the output voltage equals the sum of the voltages produced by both elements, and the output characteristics resemble those of a 1S connection. In contrast, when three elements were linked in series which in a 3S connection, the output voltage was equal to the sum of the three voltages, and the output characteristics showed a similar pattern. For all connection configurations, the results presented in Tables 1, 2, and 3 show that greater speeds produced higher output values, whereas lower speeds produced lower output values.

Table 1 1S Output

Speed (%)	Voltage (V)	Power (mW)
40	1.55	0.24
50	2.22	0.49
60	3.15	0.99

Table 2 2S Output

Speed (%)	Voltage (V)	Power (mW)
40	2.46	0.30
50	3.46	0.60
60	4.21	0.89

Table 3 3S Output

Speed (%)	Voltage (V)	Power (mW)
40	2.80	0.26
50	5.32	0.94
60	6.72	1.50

3.1.2 Parallel of Piezoelectric Configuration System Experimental Result

This experiment determined two different topologies of parallel connections using piezoelectric devices. The voltage output remains constant as a result of the combined currents of the parallel elements. This produces more power output as compared to a single element. Table 4 shows that, at various speeds, the output voltage, and power are, accordingly minimum at 40% speed and highest at 60% speed. Comparably, in a 3P connection, increasing the power output while maintaining the same voltage output. Table 5 shows that the output parameters have a similar pattern to the 2P configuration. Lower speeds result in lower output values in both combinations, while higher speeds result in higher output values.

Table 4 2P Output

Speed (%)	Voltage (V)	Power (mW)
40	1.73	0.60
50	2.36	1.12
60	3.16	2.00

Table 5 3P Output

Speed (%)	Voltage (V)	Power (mW)
40	1.80	0.97
50	2.46	1.82
60	3.23	3.12

3.1.3 Multi-array of Piezoelectric Configuration System Experimental Result

A 2S-1P connection consists of two piezoelectric devices connected in series, followed by a single element connected in parallel. The voltage output is the total of the voltages of the elements that are coupled in series. Table 6 shows that the voltage and power output values were lowest at 40% speed and greatest at 60% speed, respectively. This shows better output power and voltage, performance at higher speeds. Then, two piezoelectric elements are connected in series with one element after being connected in parallel with one another in a 2P-1S connection. In Table 7, the voltage output is the same for all three series-connected elements. In the same way, the voltage and power output numbers were lowest at 40% speed and greatest at 60% speed. Once more, increased speeds led to better output power and voltage performance.

Table 6 2S-1P Output

Speed (%)	Voltage (V)	Power (mW)
40	1.61	0.52
50	2.37	1.12
60	3.47	2.40

Table 7 2P-1S Output

Speed (%)	Voltage (V)	Power (mW)
40	2.27	0.26
50	4.56	1.04
60	6.15	1.89

3.1.4 Overlapping of Piezoelectric Configuration System Experimental Result

Table 8 displays the power and output voltage for the 3S-PO connection after testing at 40%, 50%, and 60% of the maximum speed. The voltage output reaches its minimum at 40% speed and its maximum at 60% speed. In a similar vein, at 40% speed the lowest numbers for power are acquired, while at 60% speed the greatest values are noted. The 3S-NO connection is next investigated in Table 9 utilizing the identical 10M ohm resistor and speed tests. Table 8 shows a similar pattern for the voltage and power outputs, with the lowest values at 40% speed and the greatest values at 60% speed. The 3P-PO connection in Table 10 is then examined using speed tests and a 10M ohm resistor. According to the preceding tables, the outputs of voltage and power are at their lowest at 40% speed and reach their highest levels at 60% speed. Finally, Table 11 shows power for a 3P-NO connection using speed testing through a 10M ohm resistor. Similar to the previous tables the power and voltage outputs show a result where the maximum values at 60% speed and the lowest values at 40% speed.

Table 8 3S-PO Output

Speed (%)	Voltage (V)	Power (mW)
40	2.60	0.23
50	4.46	0.66
60	6.72	1.50

Table 9 3S-NO Output

Speed (%)	Voltage (V)	Power (mW)
40	1.37	0.06
50	2.36	0.19
60	3.88	0.50

Table 10 3P-PO Output

Speed (%)	Voltage (V)	Power (mW)
40	1.01	0.30
50	2.12	1.35
60	2.95	2.61

Table 11 3P-NO Output

Speed (%)	Voltage (V)	Power (mW)
40	0.76	0.17
50	1.62	0.79
60	2.65	2.11

3.2 Discussion

The output voltage and power outputs for different piezoelectric setups are shown in the graphs in Figures 21 and 22. It is frequently observed that the 3P design produces the highest output voltage, while the 3S arrangement delivers the highest output power. When examining the voltage output at various speeds, the 2P-1S setup exhibits a drop in increment as the speed increases, while the 3S arrangement displays an increase. A smaller rise in voltage output is also shown by the 3S-PO arrangement. Whenever compared to other arrangements, the 3P design consistently produces the maximum power output. Proving the advantages of the overlap connection, the 3P-PO arrangement exhibits the maximum power output of all the overlapping configurations. Overall, these results advance our knowledge of the functionality and effectiveness of piezoelectric energy harvesting technologies.

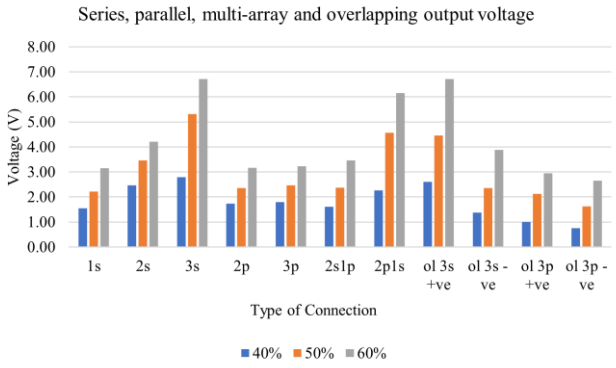

Figure 21 Configuration Output Voltage

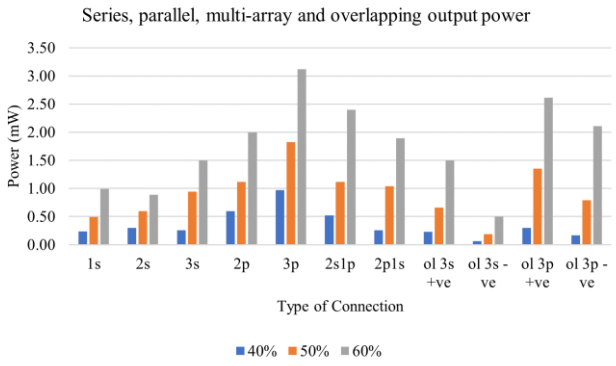

Figure 22 Configuration Output Power

4.0 CONCLUSION

Conclusively, the research's goals were accomplished by designing a variety of piezoelectric arrays configuration, arranging overlapping connections for energy harvesting, and conducting comprehensive assessments of output voltage, current, and power. Experiments conducted with this arrangement provide valuable insights into the system's performance and efficiency. This new information opens up new approach for piezoelectric energy harvesting device research and development. Creating a piezoelectric system with motors, sensors and connecting boards is the research's requirement for configuration control. Important measurements of the experiment's output voltage and power were made. The performance differences between various setups are highlighted, and their impact on energy harvesting efficiency is explained through analysis and discussion. The overall objective of this research is to increase understanding of piezoelectric energy harvesting and its potential for producing sustainable energy. According to the data, the 3S-PO configuration outperforms the overlapping configurations with the maximum voltage. In comparison to other designs, the voltage output at 40% speed exhibits an incredible rise of 70.91%. Similarly, at 60% speed, the output voltage of the 3S-PO arrangement increased by 63.68%, respectively. With the 3P-PO arrangement, the maximum power output is achieved at 40% and 60% speed, respectively, exhibiting an increase of 80% and 85.73%. These results show the usefulness of overlapping connections for effective energy harvesting applications.

Acknowledgement

The authors are grateful to Universiti Malaysia Perlis (UniMAP), particularly the Faculty of Electrical Engineering & Technology and the Centre for Graduate Studies (CGS), for their generous provision of research facilities. Special thanks to Majlis Amanah Rakyat (MARA) for their invaluable scholarship support.

Conflicts of Interest

The author(s) declare(s) that there is no conflict of interest regarding the publication of this paper.

References

[1] M. H. Alsharif, S. Kim, and N. Kuruoğlu. 2019. Energy Harvesting Techniques for Wireless Sensor Networks/Radio-Frequency Identification: A Review. Symmetry. 11(7). Doi: https://doi.org/10.3390/sym11070865.

[2] A. Mohanty, S. Parida, R. K. Behera, and T. Roy. 2019. Vibration Energy Harvesting: A Review. *Journal of Advanced Dielectrics*. 9(4). Doi: https://doi.org/10.1142/S2010135X19300019.

[3] I. Izadgoshasb, Y. Y. Lim, R. V. Padilla, M. Sedighi, and J. P. Novak. 2019. Performance Enhancement of a Multiresonant Piezoelectric Energy Harvester for Low Frequency Vibrations. *Energies (Basel)*. 12(14). Doi: https://doi.org/10.3390/en12142770.

[4] V. Pakrashi, G. Marano, P. Cahill, S. F. Ali, and M. Magno. 2018. Vibration Energy Harvesting for Monitoring Dynamical Systems. *Shock and Vibration*. Doi: https://doi.org/10.1155/2018/8396029.

[5] W. Shi, C. Yang, H. Zhao, C. Chen, Y. Gao, and X. Luo. 2023. Design, Simulation and Experiment for a Piezoelectric Energy Harvester based on Fluid Pressure Pulsation In Water Hydraulic System. *Ocean Engineering*. 288: 116097. Doi: https://doi.org/10.1016/j.oceaneng.2023.116097.

[6] A. Hosseinkhani, D. Younesian, P. Eghbali, A. Moayedizadeh, and A. Fassih. 2021. Sound and Vibration Energy Harvesting for Railway Applications: A Review on Linear and Nonlinear Techniques. *Energy Reports*. 7: 852–874. Doi: https://doi.org/10.1016/j.egyr.2021.01.087.

[7] B. Debnath, R. Kumar, and P. Mohamed Shakeel. 2020. Meandering-trapezoidal Shaped MEMS Structure for Low Frequency Vibration based Energy Harvesting Applications. *Sustainable Energy Technologies and Assessments*. 42. Doi: https://doi.org/10.1016/j.seta.2020.100881.

[8] S. Wang. 2021. Sports Training Monitoring of Energy-saving IoT Wearable Devices based on Energy Harvesting. *Sustainable Energy Technologies and Assessments*. 45. Doi: https://doi.org/10.1016/j.seta.2021.101168.

[9] A. Tabesh and L. G. Fréchette. 2010. A Low-power Stand-alone Adaptive Circuit for Harvesting Energy from a Piezoelectric Micropower Generator. *IEEE Transactions on Industrial Electronics*. 57(3): 840–849. Doi: https://doi.org/10.1109/TIE.2009.2037648.,

[10] S. Priya *et al*. 2019. A Review on Piezoelectric Energy Harvesting: Materials, Methods, and Circuits. *Energy Harvesting and Systems*. 4(1): 3–39. Doi: https://doi.org/10.1515/ehs-2016-0028.

[11] S. Panda *et al*. 2022. Piezoelectric Energy Harvesting Systems for Biomedical Applications. Nano Energy. 100(April): 107514. Doi: https://doi.org/10.1016/j.nanoen.2022.107514.

[12] D. Zhao, J. Zhou, T. Tan, Z. Yan, W. Sun, and J. Yin. 2021. Hydrokinetic Piezoelectric Energy Harvesting by Wake Induced Vibration. *Energy*. 220: 119722. Doi: https://doi.org/10.1016/j.energy.2020.119722.

[13] A. C. Turkmen and C. Celik. 2018. Energy Harvesting with the Piezoelectric Material Integrated Shoe. *Energy*. 150: 556–564, DOI: https://doi.org/10.1016/j.energy.2017.12.159.

[14] N. H. H. A. Talib, H. Salleh, B. D. Youn, and M. S. M. Resali. (2019). Comprehensive Review on Effective Strategies and Key Factors for High Performance Piezoelectric Energy Harvester at Low Frequency. International Journal of Automotive and Mechanical Engineering. 16(4): 7181–7210. Doi: 10.15282/ijame.16.4.2019.03.0537.

[15] R. R. Chand and A. Tyagi. 2022. Investigation of the Effects of the Piezoelectric Patch Thickness and Tapering on the Nonlinearity of a Parabolic Converging Width Vibration Energy Harvester. *Journal of Vibration Engineering and Technologies*. 10(1). Doi: https://doi.org/10.1007/s42417-021-00359-x.

[16] E. L. Pradeesh and S. Udhayakumar. 2019. Effect of Placement of Piezoelectric Material and Proof Mass on the Performance of Piezoelectric Energy Harvester. *Mech Syst Signal Process*. 130: 664–676. Doi: https://doi.org/10.1016/j.ymssp.2019.05.044.

[17] S. A. Kouritem, M. A. Al-Moghazy, M. Noori, and W. A. Altabey. 2022. Mass Tuning Technique for a Broadband Piezoelectric Energy Harvester Array. *Mech Syst Signal Process*. 181(February): 109500. Doi: https://doi.org/10.1016/j.ymssp.2022.109500.

[18] S. S. Kumar. 2014. Design and Simulation of Micro Resistor Beam using COMSOL. *International Journal of Advanced Scientific Engineering and Technological Research* (IJASETR). 2(1): 1–7.

[19] N. Uddin, S. Islam, J. Sampe, S. H. M. Ali, and M. S. Bhuyan. 2017. Design and Simulation of Piezoelectric Cantilever Beam based on Mechanical Vibration for Energy Harvesting Application. *2016 International Conference on Innovations in Science, Engineering and Technology*, ICISET 2016. Doi: https://doi.org/10.1109/ICISET.2016.7856532.

[20] J. Ghazanfarian, M. M. Mohammadi, and K. Uchino. 2021. Piezoelectric Energy Harvesting: A Systematic Review of Reviews. *Actuators*. 10(12): 1–40. Doi: https://doi.org/10.3390/act10120312.

[21] A. Aabid *et al.* 2021. A Systematic Review of Piezoelectric Materials and Energy Harvesters for Industrial Applications. *Sensors*. 12: 1–27. Doi: https://doi.org/10.3390/s21124145.

[22] M. R. Sarker, S. Julai, M. F. M. Sabri, S. M. Said, M. M. Islam, and M. Tahir. 2019. Review of Piezoelectric Energy Harvesting System and Application of Optimization Techniques to Enhance the Performance of the Harvesting System. *Sens Actuators A Phys*. 300: 111634. Doi: https://doi.org/10.1016/j.sna.2019.111634.

[23] A. Pop-Vadean, P. P. Pop, T. Latinovic, C. Barz, and C. Lung. 2017. Harvesting Energy an Sustainable Power Source, Replace Batteries for Powering WSN and Devices on the IoT. *IOP Conf Ser Mater Sci Eng*. 200: 1. Doi: https://doi.org/10.1088/1757-899X/200/1/012043.

[24] F. Laumann, M. M. Sørensen, R. F. Jul Lindemann, T. M. Hansen, and T. Tambo. 2017. Energy Harvesting through Piezoelectricity - Technology Foresight. *Energy Procedia*. 142: 3062–3068. Doi: https://doi.org/10.1016/j.egypro.2017.12.445.

[25] M. R. Sarker, S. Julai, M. F. M. Sabri, S. M. Said, M. M. Islam, and M. Tahir. 2019. Review of Piezoelectric Energy Harvesting System and Application of Optimization Techniques to Enhance the Performance of The Harvesting System. *Sensors and Actuators, A: Physical*. 300. Doi: https://doi.org/10.1016/j.sna.2019.111634

[26] R. Bonin, E. C. Zenerino, A. Tonoli, N. Amati, and A. Rapisarda. 2013. Model and Design of a Double Frequency Piezoelectric Resonator. 6th ECCOMAS Conference on Smart Structures and Materials. June: 24–26.